ISSN 1392–1320 MATERIALS SCIENCE (MEDŽIAGOTYRA). Vol. 20, No. 4. 2014

Influence of Terahertz Waves on Unidirectional Carbon Fibers in CFRP Composite Materials

Kwang-Hee IM [1] *, David Kuei HSU [2], Chien-Ping CHIOU [2], Daniel J. BARNARD [2], Sun-Kyu KIM [3], Sung-Jun KANG [3], Young-Tae CHO [4] , Jong-An JUNG [5], In-Young YANG [6]

[1] *Department of Mechanical and Automotive Engineering, Woosuk University, Jeonbuk, 565-701, Korea*
[2] *Center for Nondestructive Evaluation, Iowa State University, Ames, Iowa, 50011, USA*
[3] *Division of Mechanical System Engineering, Chonbuk Natl. University, Jeonbuk , 561-756, Korea*
[4] *Department of Manufacturing Design Engineering, Jeonju University, Jeonju, 560-759, Korea*
[5] *Department of Mechanical and Automotive Engineering, Songwon University, Kwangju 502-210, Korea*
[6] *Department of Mechanical Design Engineering, Chosun University, Kwangju 501-759, Korea*

crossref http://dx.doi.org/10.5755/j01.ms.20.4.6440

Received 13 February 2014; accepted 26 November 2014

Terahertz time domain spectroscopy (THz TDS) system based on the reflective and through-transmission modes was utilized. Influence of terahertz waves (T-ray) on the fiber surface layups in the CFRP solid composites was studied. It was found that the value of electrical conductivity in the carbon fibers varies by the layup directions of carbon fibers based on E-field (Electrical field). T-ray optimized scanning data could be obtained at the 90° angle normal to the E-field direction. GFRP (Glass-fiber reinforced plastics) composite laminates were scanned with two saw cuts using a T-ray THz TDS system and the terahertz optimized scanning images were obtained at the angles normal to the E-field direction on the nonconducting materials. Also, by use of 2-dimensional spatial Fourier transform, interface C-scan images were transformed into quantitative angular distribution plots in order to show the fiber orientation information therein and to make the orientation of the ply predictable.

Keywords: terahertz waves, unidirectional CFRP composites, carbon fiber, reflection, transmission mode.

1. INTRODUCTION

It is well known that terahertz zone lies somewhere between microwave and infrared zone of electromagnetic spectrum (EM). Also, the advanced techniques and detecting system today in terahertz technology was successful to provide an authenticate range on the EM (electromagnetic spectrum). The terahertz radiation, which has pretty lower attenuation, shorter wavelength and relatively greater resolution seems to highly be important in the spectroscopy valuation of critical medical imaging, security checks in airport, water/toxic materials and advanced composite parts [1 – 6]. This can bring 1/12 (pico) second bursts of terahertz radiation generated and so is possible for detecting defects with using higher resolution eventually.

The technology of terahertz "T-ray" is comprising imaging, signal processing techniques and detecting techniques to analyze scanning images of defects in composites [7]. Because of its broad zone of simplicity and utilizations of the technology, the terahertz system has the potential of being the priority choice of THz-TDS scanning system as very small / light and safe means in field applications.

In this work, some of concerned applications of THz-TDS techniques were studied in order to nondestructively evaluate defects of fiber reinforced plastics (FRP) solid composites and structural parts. In those works, the scanning techniques were employed as two ways with both reflective and through-transmission configurations, for which T-ray pulses were set up for building up data images. Measuring techniques of refraction indices were deeply investigated in an attempt to use for resolving on the reflective and through-transmission configurations. The composite materials and structures used in this work include both polymeric composites with non-conducting property reinforced by Kevlar and glass, and carbon fiber composites with conducting property respectively. The structures used in the experiments were honeycomb or foam core sandwiches and glass fiber reinforced plastics / carbon fiber reinforced plastics (GFRP/CFRP) solid laminates. The penetration ability of T-ray waves has a limit in the conducting carbon fiber composites. The experiment of THz TDS testing was conducted extensively on CFRP laminate at different angles against E-field. Accordingly, the influence and limitation of terahertz radiation on NDE directions of the composites were discussed. THz scan images could be effectively made with respect to the angles of orientation of carbon fibers. It follows the general understanding that the contrast of images is influenced higher by the E-field direction. T-ray C-scan images were also obtained and 2-D FFT was utilized for obtaining the fiber direction information and predicting the ply orientation.

2. THEORY AND EXPERIMENT

2.1. System set up

The T-ray advanced system utilized in our work was manufactured by Tera View Ltd. Co. as shown in Fig. 1, which includes a pulsed system of time domain spectroscopy (TDS). The spatial resolution could be

*Corresponding author. Tel.: +82-63-290-1473; fax.: +82-63-291-9312.
E-mail address: *khim@woosuk.ac.kr* (K. H. Im)

determined by the T-ray spot size using the focused lens. General resolution is ranged from 0.3 mm to 1.0 mm in this T-ray system. Frequency in the THZ TDS system is ranged from 50 GHz to 4 THz and a delay time was limited to 300 ps. Focal lengths of THZ beam are composed for both 50 mm and 150 mm. Fig. 1 shows a schematic of T-ray system with the mode configurations [8], which includes a laser transmitter, an optical delay line, current preamplifiers and T-ray beams.

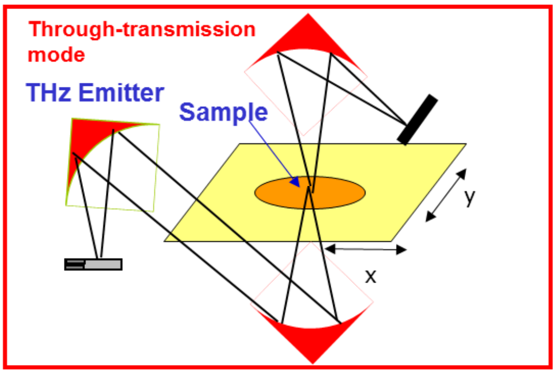

Fig. 1. Terahertz advanced system for making images

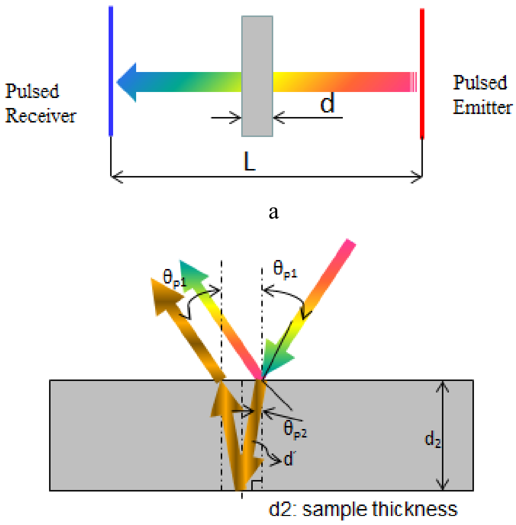

b

Fig. 2. Measuring refractive indices: a – through-transmission mode; b – reflective mode

2.2. Measurement techniques

Indices of refraction can be concerned as a parameter of properties for evaluating materials as shown in Fig. 2. Accordingly, the authors are suggesting a procedure for evaluating the electromagnetic properties including index of refraction. Indices of refraction (n) for both through-transmission and reflection configurations could be obtained by equations both (1) and (2) below.

This method is intended for determining the indices of refraction that is utilized to solve the difference of passing lengths between the front side and back-wall reflective waves in the domain of time. Fig. 2 is plotted for the geometry when the THz waves are passing in the samples. The refractive index (n) [3] is now defined by:

$$n = 1 + (\Delta t \cdot v_{air}/d)\,; \qquad (1)$$

$$n^4 - An^2 - A\sin^2\theta_{p1} = 0, \text{ where } A = (T^2 V_{air}^2)/(4d_2^2); \qquad (2)$$

here, T is the through-transmission time in the sample, d is the thickness of samples in the through-transmission mode, V_{air} is the light velocity in air, d_2 is the sample thickness in refraction mode, θ_{p1} is the inclined angle in samples, Δt is the difference of time between sample and no-sample, and L is the length between pulse emitter and pulse receiver.

3. DISCUSSION AND RESULTS

3.1. Measuring indices of refraction

In order to obtain a parameter of materials, THz pulses reflected from GFRP composites were measured first of all. Fig. 3 shows clearly the first signal reflected from the top surface and then the subsequent signal reflected from the back-wall surface in glass fiber composites. Method for determining the indices of refraction was utilized to solve the passing lengths between the front side and back-wall reflective waves as shown in Table 1. It was confirmed that these data corresponded well with the previous results using the T-ray techniques [9]. However it appears that there is some difference between through-transmission mode and reflection mode in case of GFRP composites due to their different properties.

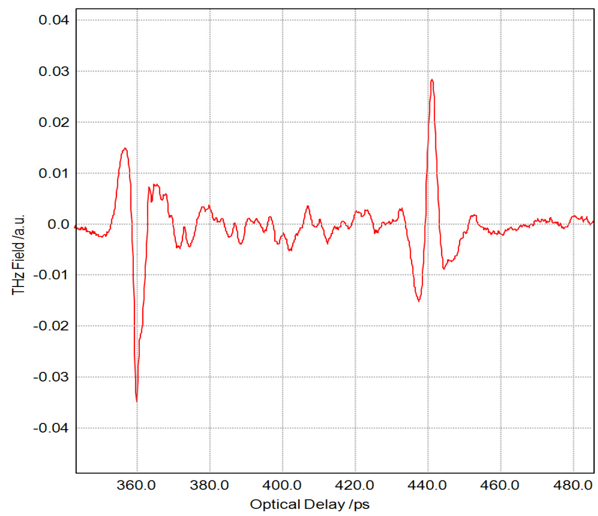

Fig. 3. Typical THz signal of the mode of refraction in glass composite laminates

Table 1. Indices of refraction in the materials

Material	Indices of refraction (n)*	Indices of refraction (n) in the current experiment	
		Mode of through transmission	Reflective mode
Fused quartz	1.95 ±0.06	1.96 ±0.03	1.96 ±0.04
GFRP	–	2.11 ±0.20	2.12 ±0.30
PMMA	1.60 ±0.08	1.59 ±0.03	2.12 ±0.04

*Previous results by Ref. [9].

3.2. Correction between E-field and the direction in carbon fiber

The THz pulsed waves could quite easily penetrate the materials with dielectric properties except the materials with electrical conduction. There are some literatures suggesting use of THz radiations on investigating carbon fiber composite materials [9, 10], however, they are insufficient in in-depth approach. CFRP composite materials are considered as pretty low conductors based on the electricity and the properties in conductivity is of anisotropy in fiber directions.

Therefore, there is worth to make effort for quantifying the degree of the THz waves how to penetrate carbon composite laminates. Usually the amount of transverse conductivity is electrically concealed by short of fiber continuity in unidirectional carbon laminates.

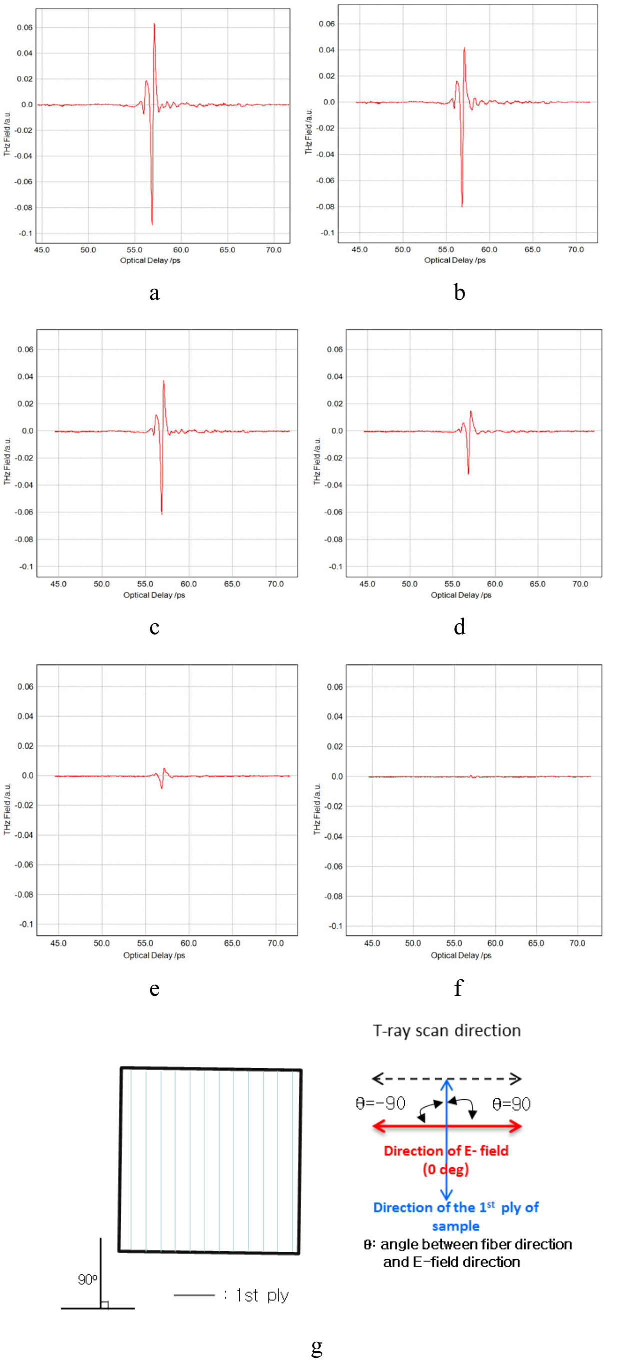

Fig. 4. Angular peak-to-peak amplitudes of through- transmission mode in a CFRP sample: a – θ = 90° scan to E-field for the 1st ply; b – θ = 75°; c – θ = 60°; d – θ = 45°; e – θ = 15°; f – θ = 0°; g – configuration for T-ray testing

The value of conduction depends on the fiber directions and also on contact degree between touching fibers. The amount degree of conductivity are very random for the carbon fiber composite materials [11]. The value of conductivity in longitudinal direction (σ_1) vary from 1×10^4 S/m to 6×10^4 S/m and the value range of the conductivity in transverse direction (σ_t) is very sparse from 2 to as great as 600 S/m. The value of conductivity in transverse direction is greatly dependent on the process and quality of manufacturing techniques in a unidirectional CFRP composite materials. In unidirectional CFRPs, the value of in-plane conductivity was provided by [12].

Due to its highly anisotropic electrical conductivity ($\sigma_1 >> \sigma_t$), penetration of terahertz waves through unidirectional CFRP composites was related with a function of angle between the vectors in both electrical field and the fiber directions. When the E-field of the THz wave is parallel to axial direction in carbon fibers, the conductivity is the highest and the penetration is the lowest. In the experiment, the authors plotted out the value of angular profile of the through-transmission waves through carbon composite materials by continuous wave instrumentation. The transmitted power was around 30 dB over the level of noise at bottom layer in frequency spectrum ($f \sim 0.1$) in Fig. 4.

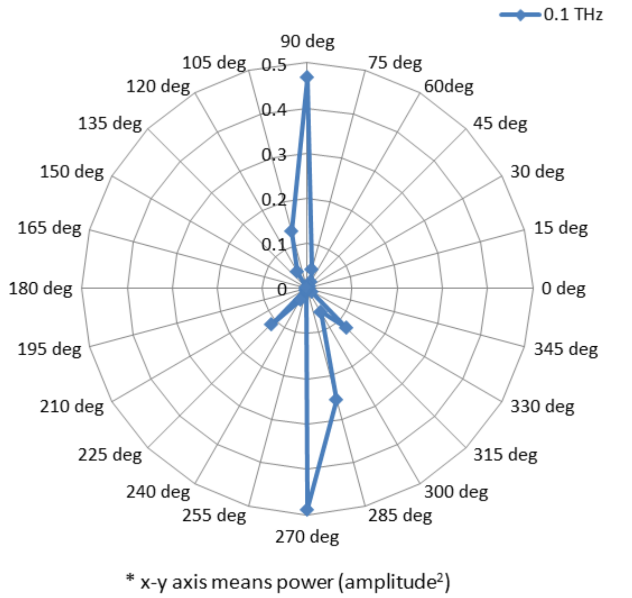

Fig. 5. Reconstructed angular profile of through-transmission mode in a CFRP sample

The transmission powers were measured at every 15 degree angles. Fig. 4, a, shows the highest transmission power amplitude, and Fig. 4, f, shows the lowest. The measured power amplitudes were plotted against angles as shown in Fig. 5. It was found that the THz waves could easily penetrate the carbon composite materials in the case of 90 degree perpendicular to the fiber axis.

3.3. Multiple delamination imaging

In T-ray pulses in the TDS system, the time domain waveform resemble to ultrasonic signals highly. It was found that the concepts of wave propagation were common in both waves such as reflection and transmission coefficients, TOF (time-of-flight), refraction and diffraction.

However, there were fundamental differences when materials were examined by various means such as terahertz radiation, electromagnetic wave and ultrasound wave. First of all THz waves, compared with ultrasonic wave never used a couplant like medium things to propagate it, and therefore could easily penetrate off either air or materials.

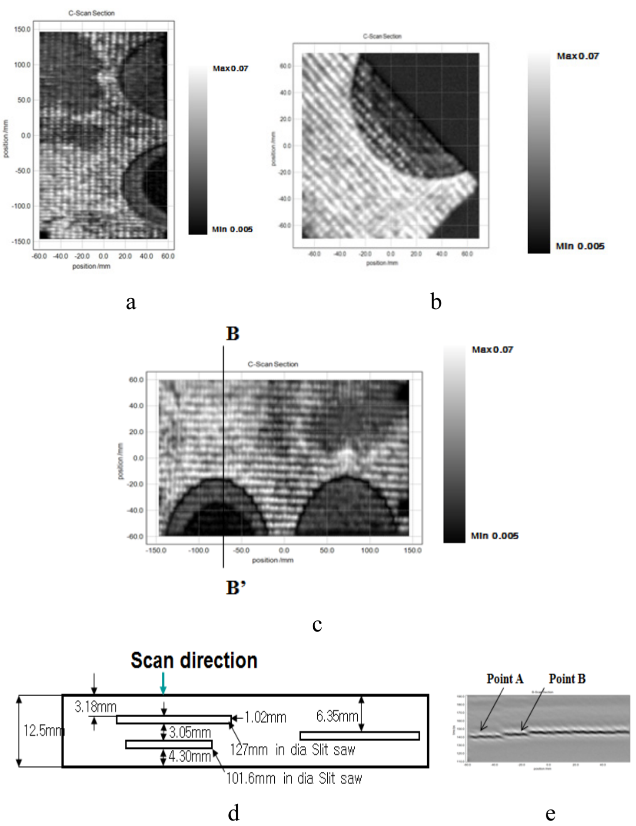

Fig. 6. Double and single saw-cut scanning images in T-ray scanning in glass fiber composites: a – θ = 90° scan to E-field; b – θ = 45°; c – θ = 90°; d – geometry; e – B-scan image at B-B’ line

In ultrasound investigation for defects in a glass carbon composites, the practical area has hardship from the “shadow effect”, where a smaller defect behind a greater defect cannot be found. By contrary, the THz waves could detect two defects without limitation. In order to show this possibility, smaller and larger saw-cuts with half-circular shapes were made in a glass composite materials (1/2 inch thick), which are simulating delaminations in Fig. 6. Fig. 6 shows THz scanning images in GFRP composite laminates with two saw cuts at the different angles (0, 45, 90 degrees) with through-transmission mode. Fig. 6, e, shows a B-scan image of B-B’ line shown in Fig. 6, c. It appears that the different color density in a scanned image agrees with the saw-cut locations (points A and B). The result indicates particularly that the THz waves do not have hardship such as a “shadow effect” and there is no fiber direction effect to the terahertz waves even if it may be non-conducting material.

3.4. T-ray scanning of embedded defects in Kevlar/Nomex sandwich

TDS terahertz scans in through-transmission and reflection configurations (small angle pitch-catch) were proven to be efficient in detecting out flaws placed between Nomex honeycomb core and Kevlar composite face sheet of a sandwiched plate. Also, THz images could be mapped out in both time domain and frequency domain FFT signal based on the peak-to-peak amplitude of the THz waves penetrated through or refracted from the plate.

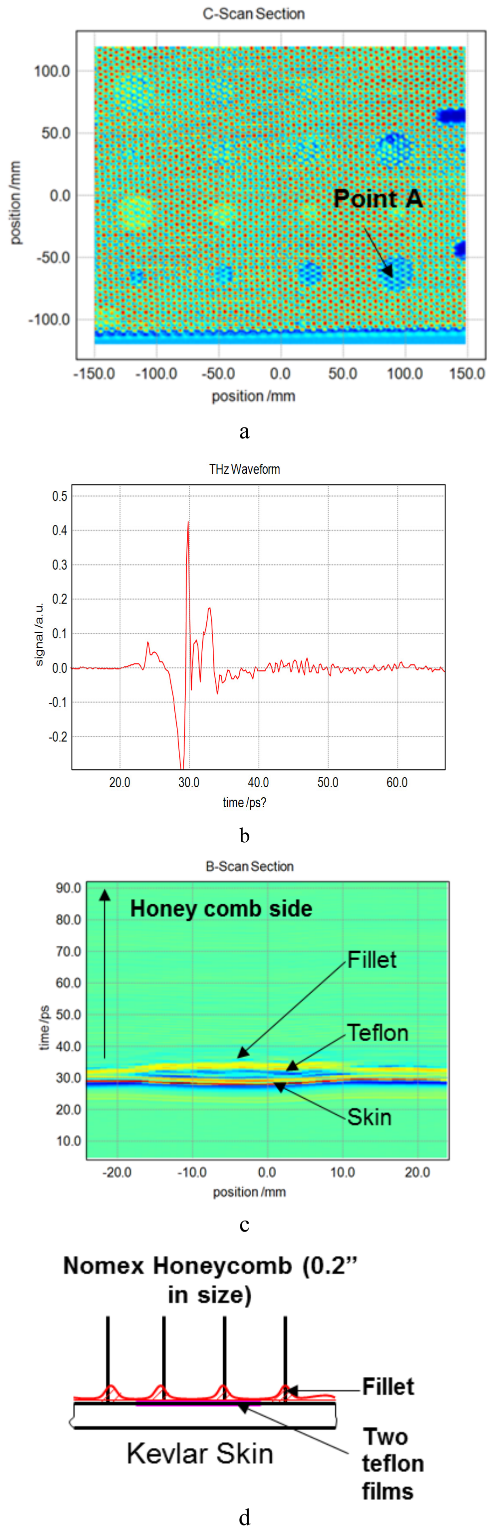

Fig. 7. Embedded defects in Kevlar/Nomex sandwich panel: a – THz scanning images with defects; b – THz signal reflected from point A; c – THz images of B-scan in horizontal middle line at point A; d – plotted drawing in front view at point A

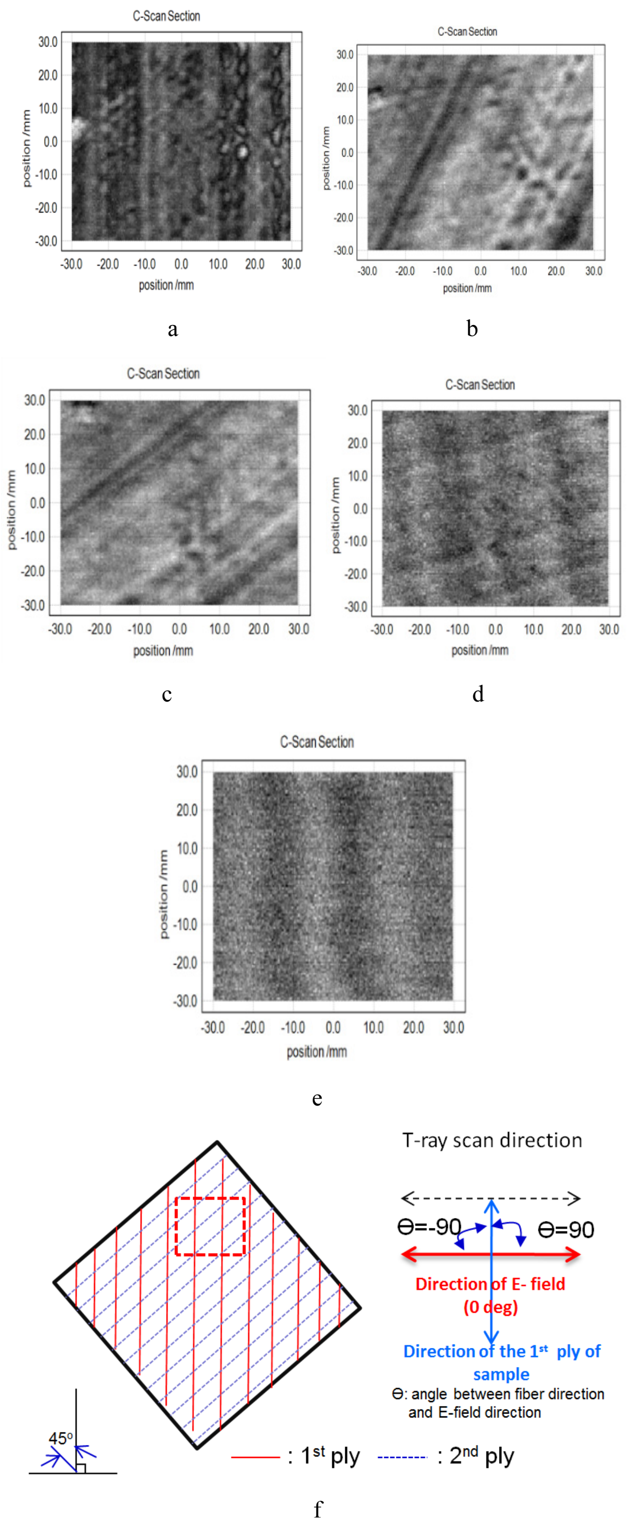

Fig. 8 Terahertz scan images with TDS reflection mode in CFRP composite laminate. (a)$\theta = 90.0^{o}$, (b)$\theta = 67.5^{o}$ (c)$\theta = 45.0^{o}$, (d)$\theta = 22.5^{o}$, (e)$\theta = 0.0^{o}$ and (f) T-ray testing arrangement

Fig. 7 shows the whole scan images with defects embedded in Kevlar/Nomex sandwich, the peak-to-peak amplitude of FFT components in the frequency domain with a gap of 0.2 THz – 0.3 THz at point A, B-scan images of the sandwich panel and reconstructed drawing of the skin and honeycomb cell joint in the sandwich. The panel has defects in the skin joint with the double-Teflon films (25.4 mm (1 inch) circle in diameter) under face sheet and with single-Teflon films (25.4 mm (1 inch) circle in diameter) on the left hand side.

3.5. Carbon fibers

Detectability of flaws in CFRP composite laminate was verified by the electrical conductivity in carbon composites. The laminate was cured in layup of $[45/0/–45/90]_{6s}$. In the top surface two plies of the CFRP laminate, the fiber orientations were –45° and 0° respectively. Fig. 8 shows THz scanning images in the laminate by using TDS T-ray waves in the reflection mode.

Fig. 8 shows that both the first and the second plies were detected from the top surface of the CFRP composite laminate. Besides, the detectability of the flaws in carbon fibers (or ratio in signal-to-noise) was dependent upon the correction between directions of the fiber and E-field form the top surface. Several THZ scanning images were made based on the "θ" angle, which means angles between fiber direction and E-field direction. Consideration must be given to the effect of interpreting the T-ray scan images of the fiber influence beneath the 1st two plies in the CFEP composites. Firstly, the penetration through the 1st two plies depends on the angle between the fiber direction and the E-field in the top 1st two plies. T-ray radiation must have transmitted through the top 1st ply, which is to penetrate the top 2nd ply. Therefore, the detectability of the fiber in the 2nd ply depends on the "θ" angle from the top surface. Since the first two plies of CFRP composite laminate were cured at the same direction, one more conducting ply could be added up below them. For this reason, the authors added up the value of conductivities of the top two plies: $\sigma_1 + \sigma_2$ and correlated the values to the S/N ratio of the defects in the T-ray image.

Consideration must be given to the effect of interpreting the T-ray scan images of the fiber influence beneath the 1st two plies in the CFEP composites. Firstly, the penetration through the 1st two plies depends on the angle between the fiber direction and the E-field in the top 1st two plies. T-ray radiation must have transmitted through the top 1st ply, which is to penetrate the top 2nd ply. Therefore, the detectability of the fiber in the 2nd ply depends on the "θ" angle from the top surface. Since the first two plies of CFRP composite laminate were cured at the same direction, one more conducting ply could be added up below them. For this reason, the authors added up the value of conductivities of the top two plies: $\sigma_1 + \sigma_2$ and correlated the values to the S/N ratio of the defects in the T-ray image.

When the "θ" angle is 90.0° angle, the value of conductivity was $0.0\,\sigma_1$ which means the lowest value assuming that $\sigma \approx \sigma_1 \cdot \cos^2\theta$. The S/N ratio in the image with fibers is therefore presumed to be the greatest when the fibers lie at this angle. On the contrary, when "θ" = 0^{o} ($\sigma = 1.0\,\sigma_1$) a carbon fiber had very lower S/N ratio, which means highest value in total conductivity. In the THZ scanning images, study of detectability influenced by fiber orientation indicates that the modeled data has very strong correlation with the experimentation qualitatively, which is also corresponding with the S/N ratio. Accordingly, a simple model 12 was utilized considering one ply to the T-ray wave based on the E-field direction. Table 2 shows conductivity values obtained in this way. In case of 0 degree to the E-field direction, the highest conductivity value was shown, which means the T-ray was blocked by the CFRP composite laminates, while, in case of 90 degree, the lowest conductivity value was shown, which means it was penetrating the CFRP composite laminates.

So, techniques of advanced scanning images were demonstrated using several samples. It was found that the influence of fiber direction that was imaged as show in Fig. 8, a, is clearly comparable to the rest of Fig. 8. However, nothing could be penetrated as shown in Fig. 8, e, because the 1st ply fiber was blocking the T-ray.

Table 2. The value of conductivity in the ply

Direction to E-field	0°	22.5°	45.0°	67.5°	90°
θ	0	22.5	45	67.5	90
σ_1	1.0	0.75	0.5	0.25	0
σ	1.0 $\cos^2\theta$	0.75 $\cos^2\theta$	0.5 $\cos^2\theta$	0.25 $\cos^2\theta$	0 $\cos^2\theta$
R_{eq}	1	0.64	0.25	0.04	0

3.6. THZ image processing on PPS CFRP solid laminate

A PPS CFRP solid laminate that was consisted with the different angles in each ply was scanned by a reflection THz-TDS system as shown in Fig. 9.

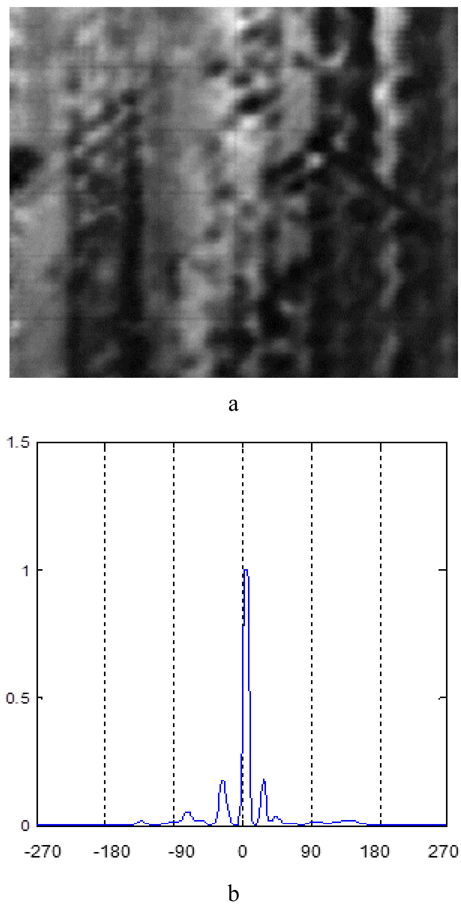

Fig. 9. Determination of the layup using 2-D FFT for θ = 45° (a) and θ = 90° (b) for the CFRP specimen [(0/45/90/–45)]: a – T-ray image; b – 2-D FFT

The scanned images show that the ply lay-up direction of the laminate was based on the "θ" angle. Since determining fiber directions of the angular components in the THz-TDS C-scan was difficult, an image simply by visual observation is given as shown in Fig. 9, a. So, the information of fiber angles required to be analyzed quantitatively is described by the angular components in the THz-TDS C-scan images. The approach taken was using a 2-dimensional fast Fourier transform (2-D FFT). An example that illustrates the image processing procedure is given in Fig. 9. The original C-scan image is shown in Fig. 9, a.

To process this image, a two-dimensional Hanning window was firstly applied to reduce the edge effects on its spatial Fourier transform. A 2-D FFT was then performed and Fig. 9, b, shows the resulting spatial spectrum where the grayscale is proportional to the magnitude of the spectrum in dB. The THz-TDS C-scan method was then used to determine the orientation of all the plies in a 48-ply laminate that had a layup of [(0/45/90/–45)]. It was confirmed that there was difference by the locations of peak amplitude in the surface of a specimen. The angular spectrum for fiber effect is shown in Fig. 9, b. Here X-axis is angle of function and Y-axis is a peak signal of ply-error location in the laminates. Take a look of Fig. 9, for example, the angular distribution plot of the first interface (between the 0° and 45° plies) shows that the highest peak is at 0° (see Fig. 9, a). This may be because of the fact that the dark dot of the images were caused from waviness of ply.

Lay-up of fiber angles could be usually determined by the THz-TDS scanning images, which contain data related with information of fiber place at different angles. It was found that variations may happen in amplitude when the THz-TDS waves go through a couple of ply of composites and, therefore, the signal change governs determination of ply-layup orientation.

4. CONCLUSIONS

Various composites were studied using a Terahertz time-domain transmission spectroscopy system. Indices of refraction in the T-ray frequency zone were measured in several materials of glass fiber composites and PMMA. Such data corresponded fairly well with the previous results with developed formulas in this study. In nondestructive testing, in conducting materials of carbon fiber composites, the penetration of T-ray wave was limited for a use of utilization in CFRP composite materials. On the contrary, in non-conducting materials of glass fiber composites, T-ray wave is able to complement conventional ultrasonic techniques such as its detectability and no hardship from "shadow effect". It was found that the terahertz waves could go through the non-conducting materials such as GFRP composites regardless of the E-field direction. The surface ply orientation of the laminates can be mapped out by performing a THZ-TDS C-scan imaging with T-ray signals reflected from the laminate and using an image processing procedure based on two-dimensional Fourier transform. Like other advanced techniques, the system cost will be reduced and portable equipment are coming out day by day and so much better procedures on THZ utilizations and applications may have to be, therefore, set up for composite NDE.

Acknowledgments

This study was sponsored by Basic Science Research Program through NRF (the National Research Foundation of Korea) funded by the Ministry of Education, Science and Technology, Republic of Korea (No. 2011-0008391).

REFERENCES

1. **Chiou, C.-P., Hsu, D.-K., Barnard, D., Im, K.-H., Thompson, R.-B.** Signal Modeling in the Far-Infrared Region for Nondestructive Evaluation Applications *Review of Progress in Quantitative Nondestructive Evaluation* 30 (1) 2011: pp. 581 – 588.
2. **Chiou, C.-P., Margetan, F.-J., Hsu, D.-K., Barnard, D., Jensen, T., Eisenmann, D.** Nondestructive Characterization of Uhmwpe Armor Materials *Review of Progress in Quantitative Nondestructive Evaluation* 31 (1) 2012: pp. 1168 – 1175.
3. **Im, K.-H., Lee, K.-S., Yang, I.-Y., Yang, Y.-J., Seo, Y.-H., Hsu, D.-K.** Advanced T-ray Nondestructive Evaluation of Defects in FRP Solid Composites *International Journal of Precision Engineering and Manufacturing* 14 (6) 2013: pp. 1093 – 1098.
4. **Gregory, I.-S., Baker, C., Tribe, W., Bradley, I.-V., Evans, M.-J., Linfield, E.-H.** Optimization of Photomixers and Antennas for Continuous-Wave Terahertz Emission *IEEE Journal of Quantum Electronics* 41 (5) 2000: pp. 717 – 728. http://dx.doi.org/10.1109/JQE.2005.844471
5. **Brown, E.-R., Smith, F. W., McIntosh, K. F.** Coherent Millimeterwave Generation by Heterodyne Conversion in Low-Temperature-Grown GaAs Photoconductors *Journal of Applied Physics* 73 (3) 1993: pp. 1480 – 1484. http://dx.doi.org/10.1063/1.353222
6. **Brown, E.-R., McIntosh, K.-A., Nichols, K.-B., Dennis, C.-L.** Photomixing up to 3.8 THz in Low-Temperature-Grown GaAs *Applied Physics Letter* 66 (3) 1995: pp. 285 – 287. http://dx.doi.org/10.1063/1.113519
7. **Mittleman, D., Jacobsen, R.-H., Nuss, M.-C.** Tray Imaging *IEEE Journal of Selected Topics Quantum Electronics* 2 1996: pp. 679 – 689. http://dx.doi.org/10.1109/2944.571768
8. **Hu, B.-B., Nuss, M.-C.** Imaging with Terahertz Waves *Optical Letter* 20 (17) 1995: pp. 16 – 1718.
9. **Naftaly, M., Miles, R.-E.** Terahertz Time-domain Spectroscopy: A New Tool for the Study of Glasses in the Far Infrared *Journal of Non-Crystalline Solids* 351 (1) 2005: pp. 3341 – 3346.
10. **Redo-Sanchez, A., Xu, N.-K.-J., Zhang, X.-C.** Damage and Defect Inspection with Terahertz Waves *Fourth International Workshop on Ultrasonic and Advanced Methods for Nondestructive Testing and Material Characterization* 1 2006: pp. 67 – 77.
11. **Hsu, D.-K.** Characterization of a Graphite/Epoxy Laminate by Electrical Resistivity Measurements *Review of Progress in Quantitative Nondestructive Evaluation* 4 (1) 1985: pp. 1219 – 1228.
12. **Tse, K.-W., Moyer, C.-A., Arajs, S.** Electrical Conductivity of Graphite Fiber-Epoxy Resin Composites *Materials Science* 49 (1) 1981: pp. 41 – 46.